
Predictive modeling of UHPC compressive strength: Integration of support vector regression and arithmetic optimization algorithm

[Liuyan Wang](#)^{*}, Lin Liu, Dong Dai, [Bo Liu](#), Zhengya Cheng

Posted Date: 8 August 2024

doi: 10.20944/preprints202408.0455.v1

Keywords: UHPC; Compressive strength; Predictive research; SVR; AOA



Preprints.org is a free multidiscipline platform providing preprint service that is dedicated to making early versions of research outputs permanently available and citable. Preprints posted at Preprints.org appear in Web of Science, Crossref, Google Scholar, Scilit, Europe PMC.

Copyright: This is an open access article distributed under the Creative Commons Attribution License which permits unrestricted use, distribution, and reproduction in any medium, provided the original work is properly cited.

Article

Predictive Modeling of UHPC Compressive Strength: Integration of Support Vector Regression and Arithmetic Optimization Algorithm

Wang Liu-yan ^{1,2,*}, Liu Lin ^{1,2}, Dai Dong ^{1,2}, Liu Bo ¹ and Cheng Zheng-ya ¹

¹ College of Architectural & Civil Engineering, Shenyang University, Shenyang 110044, China

² Shenyang Key Laboratory of Safety Evaluation and Disaster Prevention of Engineering Structures, Shenyang 110044, China

* Correspondence: w.ly428@163.com

Abstract: Based on an in-depth analysis of the factors influencing the compressive strength of ultra-high performance concrete (UHPC), this study examined the impact of both single factors and combined factors on UHPC performance using experimental data. The correlation analysis indicates that cement content, water content, steel fiber, and fly ash significantly affect the strength of UHPC, whereas silica fume, superplasticizers, and slag powder have a relatively smaller influence. This analysis provides a scientific basis for model development. Furthermore, the support vector regression (SVR) model was optimized using the arithmetic optimization algorithm (AOA). The superior performance and computational efficiency of the AOA-SVR model in predicting UHPC compressive strength were validated. Compared to SVR, support vector machine (SVM), and other single models, the AOA-SVR model achieves the highest R^2 value and the lowest error rates. The results demonstrate that the optimized AOA-SVR model possesses excellent generalization ability and can more accurately predict the compressive strength of UHPC.

Keywords: UHPC; compressive strength; predictive research; SVR; AOA

1. Introduction

In the increasingly specialized field of construction materials science, ultra-high performance concrete (UHPC) represents a significant advancement. Renowned for its exceptional strength and durability, UHPC offers substantial advantages over conventional concrete, making it a preferred choice for contemporary engineering projects where performance and longevity are critical [1]. However, accurately predicting the mechanical properties of UHPC, particularly its compressive strength, remains a significant challenge ^{Error! Reference source not found.}. This challenge is crucial not only for ensuring the design and structural integrity of buildings and infrastructure but also for reducing costs and enhancing the sustainability of construction practices ^{Error! Reference source not found.}. Shi et al. [4] believed that the amount of fiber could improve its mechanical properties and reduce the autologous contraction of UHPC.

The pursuit to develop accurate predictive models for the compressive strength of UHPC has driven the investigation of diverse computational approaches ^{Error! Reference source not found.}^{Error! Reference source not found.}. Among these, artificial neural networks (ANNs) have gained prominence for their capacity to mimic human learning mechanisms ^{Error! Reference source not found.}. In materials science, ANNs have proven highly effective in simulating complex behaviors, owing to their self-learning, self-organizing, and adaptive properties. These capabilities allow ANNs to capture complex patterns and model nonlinear relationships within large datasets, surpassing the capabilities of traditional statistical methods. Nonetheless, ANNs face challenges such as overfitting, opacity in their decision-making processes, and the requirement for extensive training data, which can compromise their stability and accuracy ^{Error! Reference source not found.}.

To address these limitations, increasing attention has been directed towards support vector regression (SVR). SVR utilizes the principles of machine learning rooted in statistical learning theory, aiming to minimize error, enhance predictive accuracy, and ensure model robustness, even when working with limited datasets^{Error! Reference source not found.}. By constructing a regression surface within a high-dimensional space, SVR effectively manages nonlinear relationships, making it particularly well-suited for forecasting complex properties such as the compressive strength of UHPC^{Error! Reference source not found.}.

The incorporation of SVR into predictive modeling marks a substantial advancement in materials science^{Error! Reference source not found.}^{Error! Reference source not found.}. Its utilization extends beyond theoretical research, offering significant practical benefits for construction projects. Improved predictive models facilitate more effective planning and quality control, optimize material formulations, and ensure that structural components adhere to safety and performance standards without excessive material use. This study aims to investigate and validate the efficacy of an optimized SVR model, enhanced through advanced algorithmic refinements, to predict the compressive strength of UHPC with greater accuracy and dependability than existing models. By bridging the divide between theoretical research and practical implementation, this research enhances predictability and, consequently, the feasibility of employing UHPC in future construction projects.

Predicting the strength of UHPC is a complex task that involves multiple variables and intricate nonlinear relationships^{Error! Reference source not found.}. Traditional predictive approaches, such as linear regression and empirical equations, often rely on simplified assumptions and linear processes, making them inadequate for accurately capturing and describing the dynamic interactions within these complex nonlinear systems^{Error! Reference source not found.}. The complexity further increases when considering projections of carbon emissions^{Error! Reference source not found.}. To address these limitations and enhance overall accuracy, the arithmetic optimization algorithm (AOA) was introduced. AOA is a novel optimization technique that improves both global and local search capabilities of the solution space through straightforward yet effective arithmetic operations^{Error! Reference source not found.}. This method is inspired by basic arithmetic principles in nature, employing multiplication and division operations to explore various regions of the solution space and refining the search direction and step size using addition and subtraction operations. This approach aims to identify hyperparameter configurations that minimize network errors.

By integrating AOA into the hyperparameter optimization process, the search for optimal hyperparameters can be both automated and expedited. This approach enhances the likelihood of identifying superior hyperparameter combinations, as AOA effectively balances exploration (global search) and development (local search). This balance ensures that the algorithm avoids local optima and progresses towards a global optimal solution^{Error! Reference source not found.}. Furthermore, employing AOA reduces the dependence on manual expertise, thereby making the model training process more efficient and automated^{Error! Reference source not found.}.

In summary, this study aims to construct an optimal prediction model, systematically analyze the correlation between key factors and prediction results, and promote the application of optimized renewable concrete in the building environment. In this paper, the support vector regression (SVR) model is optimized by arithmetic optimization algorithm (AOA). The superior performance and computational efficiency of the AOA-SVR model in predicting the compressive strength of UHPC were verified, and the prediction results were compared and comprehensively analyzed.

2. The Feasibility Analysis of the SVR Model Optimized by the AOA Algorithm

UHPC involves multiple variables and complex nonlinear relationships. It requires considering not only the composition of the concrete but also the interactions between these components and their combined effects on the final strength, making UHPC strength prediction challenging. Traditional prediction methods, such as linear regression and empirical formulas, are based on simplified assumptions and struggle to accurately describe complex nonlinear relationships. Additionally, predicting carbon emissions further complicates the process, as it involves considering the energy

consumption of raw material production, environmental impacts during production, and the lifespan of the materials, encompassing multiple dimensions.

To address these challenges, methods capable of handling highly nonlinear problems, such as ANN and SVM, are needed. These methods improve prediction accuracy by learning complex patterns and relationships within data and can self-optimize as new data becomes available. Particularly support vector regression (SVR), has been widely used to solve complex nonlinear problems due to its unique design, which effectively captures and models nonlinear relationships in data. However, the performance of ANN is heavily influenced by hyperparameter settings, which must be determined before training, making the process complex and subjective.

To overcome these limitations and improve hyperparameter optimization efficiency and model accuracy, the Arithmetic Optimization Algorithm (AOA) is introduced. AOA explores different regions of the solution space through multiplication and division operations and fine-tunes the search direction and step size using addition and subtraction operations to find hyperparameter configurations that minimize network error. The application of AOA not only automates and accelerates the hyperparameter search process but also increases the likelihood of finding optimal hyperparameter combinations. This is because AOA effectively balances exploration (global search) and exploitation (local search), ensuring the algorithm can escape local optima and progress toward a global optimal solution.

In summary, applying AOA for hyperparameter optimization, combined with the nonlinear modeling capabilities of the SVR model, provides an efficient and accurate solution for complex problems. This integration is expected to enhance the performance of AI models across various fields. In this study, we propose the AOA-SVR model by combining AOA's parameter optimization with the SVR model's ability to extract nonlinear information to capture the relationships between factors affecting mechanical performance and to predict trends in mechanical properties. The process flowchart is illustrated in Figure 1.

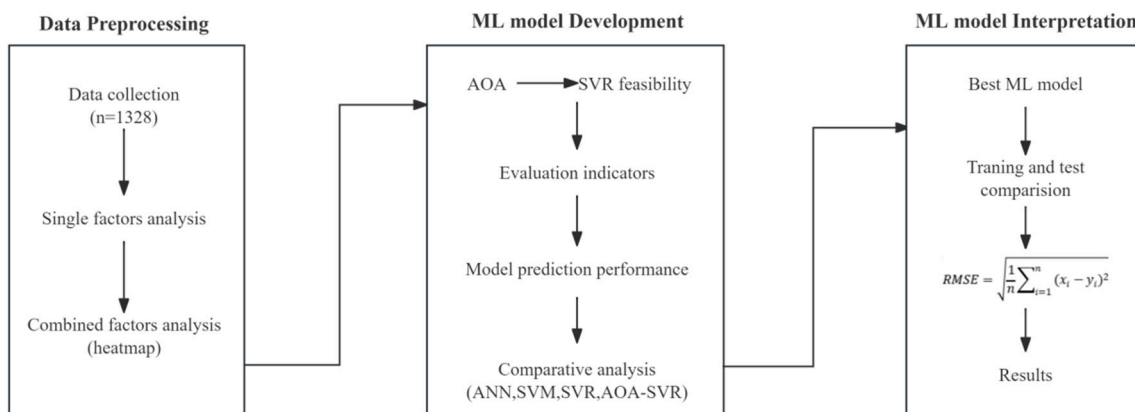


Figure 1. Working program for the establishment of the Machine learning optimization model.

3. Selection of Input Variables for Influencing Factors of Mechanical Properties of UHPC

3.1. Analysis of the Influence of Single Factors on the Compressive Strength of UHPC

This section employs the heatmap method in Python to analyze the correlation between various input variables and the compressive strength of concrete, as illustrated in Figure 2. This technique visually represents the degree of correlation between variables using an intuitive heatmap. The heatmap visually represents the correlation matrix, where each cell's color intensity signifies the strength and direction of the correlation between two variables. A darker shade indicates a stronger correlation. This graphical representation aids in identifying key predictors and understanding their relationships, thus enhancing the predictive modeling process for UHPC compressive

strength. Through detailed heatmap analysis, seven key variables were identified as having the most significant impact on the predictive model for concrete compressive strength: water content, cement content, steel fiber content, superplasticizers content, fly ash content, silica fume content, and slag powder content. This identification allows for the optimization of the predictive model and significantly enhances its accuracy.

The use of color in the heatmap clearly shows the correlation values between different variables. The correlation between water and cement usage is the most significant ($R = 0.5$), which is consistent with previous research findings. Additionally, there is a notable strong correlation between the fly ash content and the cement content, as the fly ash content directly affects the compressive strength of UHPC. Regarding the correlation between the input and output variables, the amount of cement exhibits the strongest correlation with compressive strength, the fibers usually has a greater effect on the increase of tensile strength and toughness, and its effect on the increase of compressive strength is less. And, the composition of the cementitious material on the compressive strength of UHPC is more obvious, if the cementitious material system with the composition of cement, silica fume, fly ash and slag, then the content of each kind of cementitious material changes will greatly affect the compressive strength of UHPC.

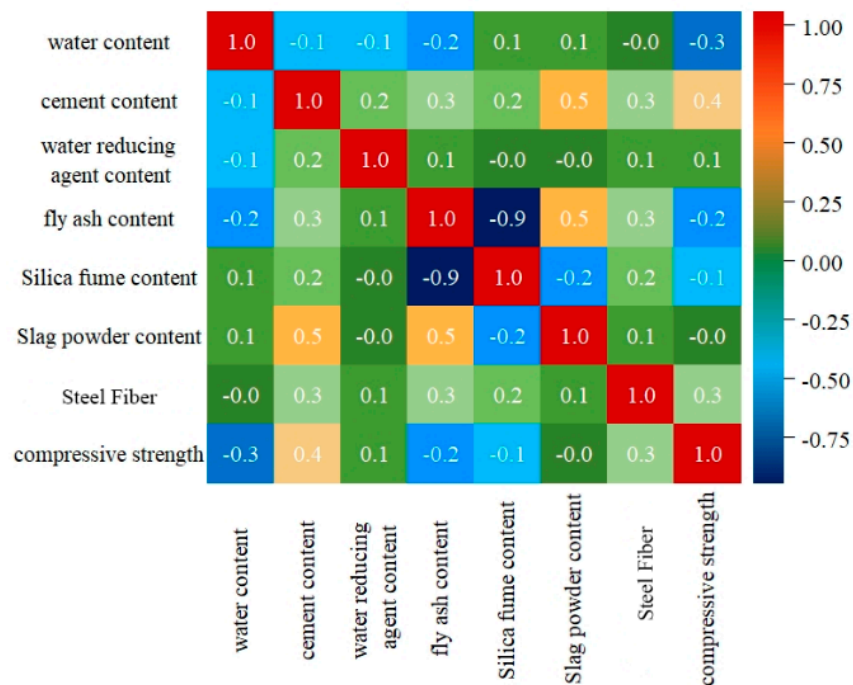


Figure 2. Heatmap of variable correlations.

Moreover, considering the significant differences in the measurement standards and numerical ranges of various variables in the original dataset, such discrepancies could adversely affect the model's performance. To mitigate this issue, we applied normalization preprocessing to both the training and testing sets before establishing the regression model. The normalization equation is as follows:

$$\bar{x} = \frac{x - \min(x)}{\max(x) - \min(x)} \quad (1)$$

where \bar{x} represents the normalized data value; x denotes the data value before normalization; and $\max(x)$ and $\min(x)$ signify the upper and lower limits of the sample data values, respectively.

After inputting the normalized values into the neural network, the output values generated by the model must also undergo inverse normalization to restore them to their original scale. The calculation method for inverse normalization is as follows:

$$\bar{y} = y(x_{\max} - x_{\min}) + x_{\min} \quad (2)$$

where y represents the output value of the neural network; x denotes the numerical value after denormalization reduction. This step eliminates the effect of range differences by scaling the data so that the values of different variables fall within the same range.

In order to study the correlation trend between various influencing factors and uhpc. We carried out related experiments with different ratios as shown in Tables 1–4.

Table 1. Effect of water-binder ratio on the compressive strength of UHPC.¹

Water-binder ratio(%)	Experimental results(MPa)		
	7d	14d	28d
0.14	288.97	324.15	335.85
0.15	294.82	328.15	338.51
0.16	299.17	333.88	342.61
0.17	307.42	337.15	351.31
0.18	311.61	341.01	355.15
0.19	317.46	347.16	359.14
0.2	321.93	352.33	363.12
0.21	315.61	341.05	355.15
0.22	310.17	335.15	348.25
0.23	302.15	331.95	340.91
0.24	299.23	328.08	333.15

¹ As illustrated in Table 1, the unique properties of UHPC are partly attributed to its extremely low water/binder ratio, which significantly enhances the compactness and strength of the concrete. Moderately increasing the water/binder ratio can mitigate internal defects and initially improve the strength of UHPC. However, an excessively high water/binder ratio reduces the efficiency of the hydration reaction, leading to a decrease in concrete strength. Therefore, identifying an optimal water/binder ratio range is crucial. This finding holds significant guiding implications for the design and application of UHPC, indicating that performance optimization can be achieved by adjusting the water/binder ratio appropriately.

Table 2. Effect of steel fiber content on the compressive strength of UHPC.²

Steel fiber (%)	Experimental results(MPa)		
	7d	14d	28d
0	280.14	302.01	327.51
0.2	283.82	308.21	333.51
0.4	287.09	312.87	338.64
0.6	292.77	316.31	343.85
0.8	294.64	320.98	347.02
1	297.31	323.05	352.78
1.2	304.12	327.04	358.15

1.4	307.22	331.61	362.71
1.6	309.42	337.02	365.56
1.8	311.61	340.45	367.61
2	312.42	342.21	368.17

² As illustrated in Table 2, steel fiber plays a crucial role in reinforcing UHPC, and an appropriate amount of steel fiber can significantly enhance its structural properties. However, as the steel fiber content increases, there are potential drawbacks. In addition to the rise in material costs, excessive steel fiber content can lead to fiber agglomeration within the concrete matrix, which adversely affects the uniformity and overall strength of the concrete. Therefore, to optimize cost-effectiveness and ensure the uniform and reliable performance of UHPC, the steel fiber content must be maintained within a reasonable range to avoid the negative effects associated with overuse.

Table 3. Effect of water reducing agent content on the compressive strength of UHPC.³

Water reducing agent(%)	Experimental results(MPa)		
	7d	14d	28d
1.4	301.01	326.46	362.13
1.5	307.23	330.58	368.14
1.6	312.01	335.21	373.74
1.7	315.21	340.25	377.58
1.8	321.46	342.65	381.14
1.9	326.47	348.25	385.14
2	324.14	343.65	378.85
2.1	317.04	337.01	371.13
2.2	311.78	332.69	367.18
2.3	307.14	329.05	362.19
2.4	300.12	326.02	357.32
2.5	297.31	323.05	352.78
2.6	292.47	317.15	349.68
2.7	286.56	314.15	345.82
2.8	283.16	310.14	340.65
2.9	279.81	306.25	336.15
3	273.67	302.12	331.13

³ As shown in Table 3, the strength of UHPC reaches a peak when the dosage of superplasticizers is optimized. However, an excessive amount of superplasticizers can increase the fluidity of the cement slurry excessively, leading to the introduction of air bubbles and segregation of the cement slurry, which ultimately reduces the overall strength of the concrete. Therefore, while water reducing agents are crucial for enhancing the performance of UHPC, their dosage must be carefully and precisely controlled.

Table 4. Effect of mineral admixtures content on the compressive strength of UHPC.⁴

Mineral admixtures(%)	Experimental results(MPa)		
	7d	14d	28d
0	299.17	322.04	349.36
10	302.16	327.66	351.21
20	307.28	335.46	355.03
30	313.14	338.74	358.14
40	316.21	341.05	362.31
50	320.18	344.15	357.17
60	318.19	340.05	354.31
70	315.24	336.91	345.48
80	311.05	332.15	341.59
90	308.82	324.51	338.21

⁴As demonstrated in Table 4, the results indicate that as the mineral admixture substitution rate gradually increases in concrete, the compressive strength of UHPC initially increases and then decreases, exhibiting a parabolic trend. At first, the incorporation of mineral admixtures enhances the strength of the concrete. However, once the substitution rate surpasses a critical threshold, the strength starts to decline. This decline occurs because mineral admixtures can dilute the concentration of the cement slurry, thereby affecting its hydration process and reducing overall strength. Thus, selecting the appropriate mineral admixture substitution rate is crucial for achieving optimal strength properties in UHPC. This parabolic relationship underscores the importance of carefully controlling the mineral admixture substitution rate during the preparation of UHPC to achieve the best possible strength results.

3.2. Analysis of the Influence of Combined Variable Factors on the Compressive Strength of UHPC

By integrating the AOA-SVR model with the grid scanning method, this study visualizes the effect of different variable factors on the compressive strength of UHPC in a three-dimensional space. This advanced analysis technique allows for the precise illustration of the combined effects of two variable factors. During the analysis, other variables are fixed at their optimal levels while observing the changes in these two variables. The results are displayed in intuitive three-dimensional graphs, each detailing how specific variations in the variable factors affect the compressive strength of the concrete.

This approach not only highlights the impact of individual variables but also provides a comprehensive analysis of how the interaction between variables jointly determines the final strength. This analysis method offers a scientific foundation for the ratio design of UHPC, aiding in the optimization of material use to achieve the desired structural performance.

As depicted in Figure 3, this subsection presents five examples that illustrate the influence of various factors on the compressive strength, serving as an important reference for the field of concrete technology.

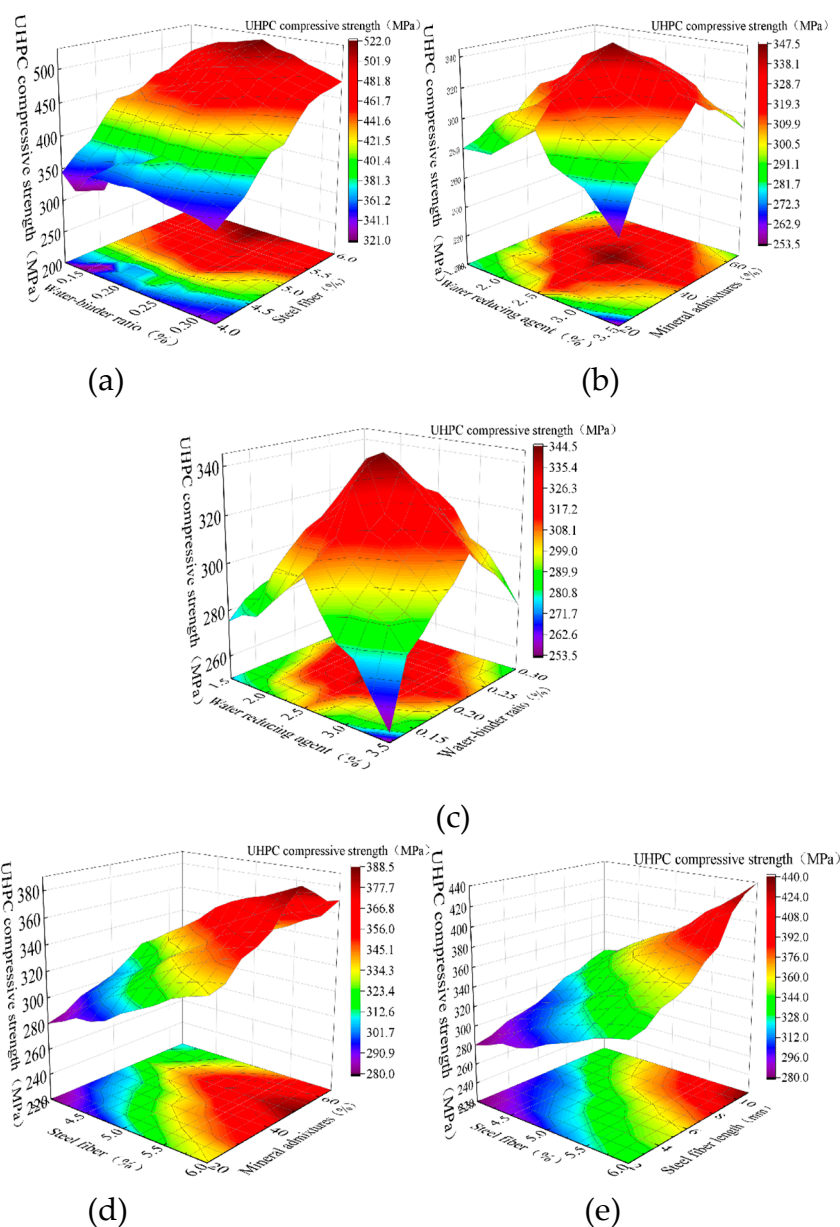


Figure 3. Three-dimensional view of the influence of combined factors on the compressive strength of UHPC.

Figure 3a illustrates the effects of the water/binder ratio and steel fiber composition on the compressive strength of UHPC. Steel fibers provide additional support and crack bridging, which can significantly increase compressive strength; however, an excessive amount can reduce the uniformity of the concrete. Similarly, while increasing the water/binder ratio can initially improve the compressive strength, an excessively high ratio can introduce too much water, thereby reducing the strength. Therefore, in preparing UHPC, it is crucial to carefully adjust the steel fiber distribution and water/binder ratio to maximize the material's advantages and prevent performance degradation.

Figure 3b demonstrates that the appropriate use of mineral admixtures and superplasticizers significantly impacts the compressive strength of UHPC. Mineral admixtures can enhance strength, particularly when used up to 40%. Superplasticizers improve workability and compactness, thus increasing compressive strength. Nevertheless, excessive use of superplasticizers may decrease strength by interfering with the normal hydration process of the cement. Therefore, moderate use of these admixtures is essential to achieve optimal compressive strength, as excessive amounts can lead to performance deterioration.

Figure 3c shows that in the preparation of UHPC, the water/binder ratio and water reducer dosage are critical factors that directly influence the compressive strength. Moderately increasing the water/binder ratio (from 0.15 to 0.20) can significantly boost strength by promoting full cement hydration and enhancing the concrete structure. However, beyond this critical value, the rate of strength increase slows down because a higher water/binder ratio increases concrete porosity. The dosage of water reducing agent was increased to 1.5%, and the strength was improved. Nevertheless, when the dosage exceeds 2.5%, the strength peaks and further increases in the water reducer dosage may lead to a reduction in strength.

Figure 3d demonstrates that the precise dosage of steel fiber and mineral admixture is crucial for optimizing the compressive strength of UHPC. As the proportion of steel fiber increases to 3.0%, the strength significantly improves, indicating an optimal proportion point. Additionally, the moderate addition of mineral admixtures can increase strength, but their positive effect diminishes after reaching a maximum value, potentially leading to a performance decline. When the steel fiber content reaches approximately 6.0%, the compressive strength initially decreases and then increases, highlighting the complex interactions between materials. Therefore, in designing UHPC, it is essential to precisely control the amounts of steel fiber and mineral admixtures to maximize performance while enhancing economic efficiency and environmental sustainability.

Figure 3e illustrates the effect of steel fiber length on the compressive strength optimization of UHPC. Considering the significant influence of the length of steel fibers on the compressive strength of UHPC^{Error! Reference source not found.}, a comprehensive investigation was conducted to explore the effect of steel fiber length on the compressive strength of UHPC. The results indicate that as the length of steel fibers increases, the compressive strength also increases. This is because longer fibers can more effectively bridge micro-cracks, enhancing the toughness and crack resistance of the concrete. However, when the steel fiber length reaches approximately 8 mm, the growth in compressive strength begins to diminish. This reduction in growth trend may be due to difficulties in the distribution and orientation of excessively long fibers within the mix. Additionally, longer steel fibers increase material costs, necessitating a balance between economic benefits and performance improvements to determine the optimal fiber length and dosage.

From the above three-dimensional diagrams, it is evident that the constructed machine learning model effectively analyzes how variations in water/binder ratio and steel fiber, mineral admixture and superplasticizers, water/binder ratio and superplasticizers, and steel fiber and mineral admixture influence the compressive strength of UHPC. This predictive analysis unveils the complex interactions among each component, providing a valuable reference for engineering applications.

4. Prediction of Mechanical Properties of UHPC Based on AOA-SVR

According to the above analysis of various factors affecting the compressive strength of UHPC, it is evident that multiple influencing factors are interrelated, and the relationship between these factors and compressive strength is complex and nonlinear. To address this complexity, machine learning technology, particularly the SVR model, is introduced into the study of UHPC. By integrating the AOA with the SVR model, researchers can scientifically predict the compressive strength of UHPC and adjust the material ratios accordingly.

This approach not only reduces the number of required experiments but also decreases research and development costs and environmental pollution. Additionally, it significantly enhances production efficiency and the stability of material properties. Therefore, the combination of machine learning and algorithm optimization, exemplified by the AOA-SVR model, offers a novel pathway for the research and application of UHPC. This method demonstrates the immense potential of modern technology in advancing the field of traditional building materials.

4.1. Preparation of Sample Data

We meticulously compiled a dataset comprising 880 samples, which were effectively divided into a training set of 700 samples and a test set of 180 samples. This partitioning strategy is designed

to thoroughly train the model using the training set and subsequently validate the model's generalization ability and predictive accuracy with the test set.

The high accuracy and flexibility of the AOA-SVR model not only provide a scientific basis for the proportion-design of UHPC but also significantly enhance the efficiency and precision of this process. The dataset includes relevant test data collected by the research team as well as trial configuration data from a civil engineering experimental testing institution, as detailed in Table 5.

Table 5. Database collections.

No.	Reference	Number of data	Proportion of data (%)
1	Song et al. ^{Error! Reference source not found.}	471	35.47
2	Graybeal, B. A. ^{Error! Reference source not found.}	294	22.14
3	Scheydt, J. C., et al. ^{Error! Reference source not found.}	72	5.42
4	Graybeal, B. A., et al. ^{Error! Reference source not found.}	59	4.44
5	Als Salman, A., et al. ^{Error! Reference source not found.}	51	3.84
6	Sobuz, H., et al. ^{Error! Reference source not found.}	40	3.01
7	Shi, Y., et al. ^{Error! Reference source not found.}	30	2.26
8	Akça, K. R., et al. ^{Error! Reference source not found.}	26	1.96
9	Ronanki, V. S., et al. ^{Error! Reference source not found.}	22	1.66
10	Fan, D., et al. ^{Error! Reference source not found.}	20	1.51
11	Als Salman, A., et al. ^{Error! Reference source not found.}	17	1.29
12	Fan, D., et al. ^{Error! Reference source not found.}	17	1.29
13	Yang, R., et al. ^{Error! Reference source not found.}	16	1.20
14	Feng, S., et al. ^{Error! Reference source not found.}	16	1.20
15	Yu, R., et al. ^[34]	12	0.90
16	Magureanu, C., et al. ^{Error! Reference source not found.}	12	0.90
17	Li, P., et al. ^{Error! Reference source not found.}	12	0.90
18	Xie, T., et al. ^{Error! Reference source not found.}	10	0.75
19	Ouyang, X., et al. ^{Error! Reference source not found.}	10	0.75
20	Alkaysi, M., et al. ^{Error! Reference source not found.}	9	0.68
21	Teichmann, T., et al. ^{Error! Reference source not found.}	9	0.68
22	Ma, J., et al. ^{Error! Reference source not found.}	9	0.68
23	Jin B K, et al. ^{Error! Reference source not found.}	9	0.68
24	Ding, M., et al. ^{Error! Reference source not found.}	7	0.53
25	Xue, J., et al. ^{Error! Reference source not found.}	7	0.53
26	Hou, D., et al. ^{Error! Reference source not found.}	7	0.53
27	Yang, R., et al. ^{Error! Reference source not found.}	6	0.45
28	Wang, X., et al. ^{Error! Reference source not found.}	6	0.45
29	Wu, Z., et al. ^{Error! Reference source not found.}	6	0.45
30	Fehling, E., et al. ^{Error! Reference source not found.}	5	0.38
31	Zhang, H., et al. ^{Error! Reference source not found.}	5	0.38
32	Arora, A., et al. ^{Error! Reference source not found.}	5	0.38
33	Ravichandran, D., et al. ^{Error! Reference source not found.}	5	0.38
34	Yu, Z., et al. ^{Error! Reference source not found.}	5	0.38

35	Su, Y., et al. <small>Error! Reference source not found.</small>	4	0.30
36	Gong, J., et al. <small>Error! Reference source not found.</small>	4	0.30
37	Wang, C., et al. <small>Error! Reference source not found.</small>	3	0.23
38	Sbia, L. A., et al. <small>Error! Reference source not found.</small>	3	0.23
39	Akhnoukh, A. K. <small>Error! Reference source not found.</small>	3	0.23
40	Farzad, M., et al. <small>Error! Reference source not found.</small>	2	0.15
41	Gu, C., et al. <small>Error! Reference source not found.</small>	1	0.08
42	Abbas, S., et al. <small>Error! Reference source not found.</small>	1	0.08
Total		1328	100%

In this subsection, 1328 test data samples from 42 literature sources were employed to train and test the machine learning model for predicting the compressive strength of UHPC. Table 1 provides detailed information on the source references, the number of data points in each reference, and the percentage contribution of each reference to the total dataset. Table 6 lists the database used in this study, which includes seven input variables utilized to construct the machine learning model. These key input parameters are water content, cement content, steel fiber content, fly ash content, silica fume content, slag powder content, and superplasticizers content. Table 6 describes in detail the minimum, maximum, mean, median, and standard deviation of these input variables.

Table 6. Database description.

	Unit	Count	Min	Max	Avg	Median	Std
Cement content	kg/m ³	1328	212.63	661.71	383.64	382.15	98.55
Water content	kg/m ³	1328	68.51	261.37	183.46	184.21	39.83
Steel fiber content	kg/m ³	1328	37.63	101.27	77.83	76.49	12.91
Fly ash content	kg/m ³	1328	200.17	656.33	329.77	331.62	91.43
Silica fume content	kg/m ³	1328	110.44	322.65	208.72	212.68	49.26
Superplasticizers content	%	1328	1.5	3.5	2.21	2.19	0.44
Slag powder content	kg/m ³	1328	87.22	266.73	169.57	171.43	39.67
Compressive strength	MPa	1328	265.21	522.79	367.56	364.97	59.36

4.2. Processing of Sample Data

In the application of the SVR model, selecting the appropriate kernel function is crucial for enhancing the model's performance. This study employs the radial basis function (RBF) as the kernel function for SVR, chosen for its capability to effectively handle nonlinear problems and capture complex patterns in data. To further boost the predictive accuracy and efficiency of the model, key parameters of the AOA-SVR model, including penalty parameters and kernel function hyperparameters, were meticulously fine-tuned. This step significantly impacts the model's performance.

Data preprocessing is a critical aspect of the machine learning process. In this study, normalization was applied to ensure that input data values fall within the range of [-1, +1]. This method effectively reduces the order of magnitude differences between different features and prevents any single dimension from disproportionately influencing the results during model training. Normalization not only accelerates the convergence speed of model training but also enhances the stability of the training process and the final generalization ability of the model.

By optimizing the parameters of the AOA-SVR model and normalizing the data, the study successfully enhances the efficiency of the model's adjustment process during training, ensuring rapid convergence to the optimal solution. This approach achieves the dual goals of efficiency and

accuracy in multiple machine learning tasks. The results demonstrate the effectiveness and reliability of the SVR model with an RBF kernel, combined with advanced parameter optimization techniques and appropriate data preprocessing strategies, in managing complex data analysis tasks.

4.3. Evaluation Indicators

To evaluate the performance of the machine learning model, this study employs five key indicators: R-squared (R^2), root mean-square error (RMSE), mean absolute error (MAE), mean absolute percentage error (MAPE) and A20-index. Among them, RMSE measures the deviation between the predicted value and the real value, and is sensitive to outliers in the data. MAE is the average of absolute errors between predicted and observed values. MAPE is used to evaluate the measurement of the error between the predicted value and the actual value. It is an important index to measure the accuracy of the predicted value. These metrics provide a comprehensive assessment of the model's accuracy and reliability. The specific equations for these indicators are provided in Table 7, with the following definitions: x_i represents the actual value; y_i denotes the predicted value; p_i symbolizes the average of the actual value; μ_i signifies the average value of the predicted value; n indicates the total number of samples in the dataset; and m_{20} is the number of samples with the ratio of experimental value to predicted value between 0.80 and 1.20.

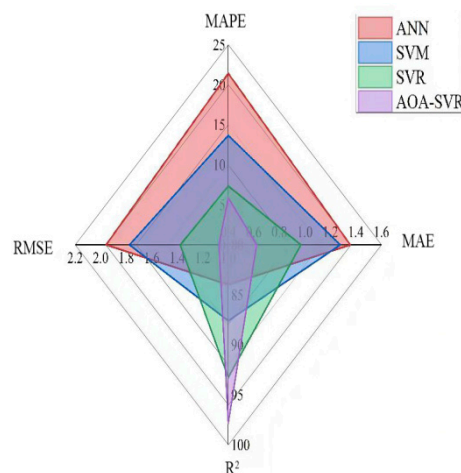
Table 7. Evaluation indicators.

Indicator	Equation	Ideal value
R^2	$R^2 = \frac{\sum_{i=1}^n (x_i - p_i)^2 - \sum_{i=1}^n (x_i - y_i)^2}{\sum_{i=1}^n (X_i - \mu_i)^2}$	1
RMSE	$RMSE = \sqrt{\frac{1}{n} \sum_{i=1}^n (x_i - y_i)^2}$	0
MAE	$MAE = \frac{1}{n} \sum_{i=1}^n x_i - y_i $	0
MAPE	$MAPE = \frac{1}{n} \sum_{i=1}^n \left \frac{x_i - y_i}{x_i} \right \times 100\%$	0
A20-index	$A20\text{-index} = \frac{m_{20}}{n}$	1

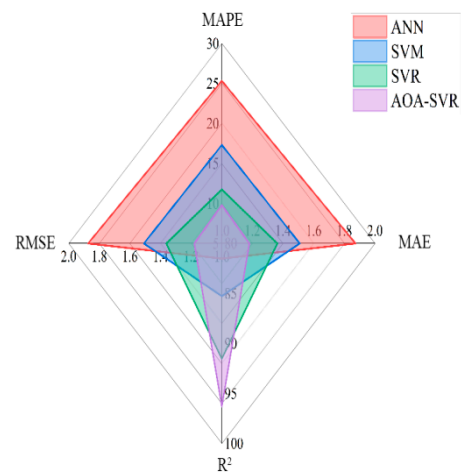
4.4. Comparative Analysis of Prediction Results

4.4.1. Model Prediction Performance and Verification Analysis

The performance indicators for the model prediction and verification analysis are illustrated in Figure 4a,b, representing the performance statistics of the training and test datasets, respectively. They clearly demonstrate that the AOA-SVR model achieves the best performance indicators across all models. Specifically, the AOA-SVR model generates higher R^2 values, while RMSE, MAE, and MAPE values are lower compared to other models. Upon combining the training phase and the test phase, the SVR model also exhibits strong performance, outperforming the other two models significantly. This indicates that, following the AOA-SVR model, the SVR model is the most reliable in predicting the compressive strength of UHPC.



(a) Training dataset



(b) Test dataset

Figure 4. Performance metrics for ANN, SVM, SVR, and AOA-SVR models.

Figure 5 displays the regression diagrams for all models during the training phase. The horizontal axis of each graph represents the observed values in the training samples, while the vertical axis represents the predicted values of the model. The black line in each figure represents perfect agreement between observed and predicted values, corresponding to the equation $y = x$. The other lines, marked by radial lines, indicate 10% and 20% deviations from the perfect agreement line. Therefore, if all points lie on the $y = x$ line, it indicates that the model can predict the actual values without any error. As shown in the figure, the AOA-SVR model not only has the highest R^2 value but also produces a regression equation closest to $y = x$. Following the AOA-SVR model in performance are the SVR, SVM, and ANN models.

While achieving high performance in the training phase is beneficial for model prediction, it does not necessarily guarantee the model's performance during the test phase. In other words, a model that performs well during training may not replicate its results during testing; therefore, their performance must be evaluated on the test data.

Figure 6 presents the regression diagrams for the models during the test phase. The AOA-SVR model demonstrates superior performance, as evidenced by the highest R^2 value and the compact

clustering of data points along the black line (the 100% consistent line). The R^2 values for the models following the AOA-SVR model are in the order of SVR, SVM, and ANN.

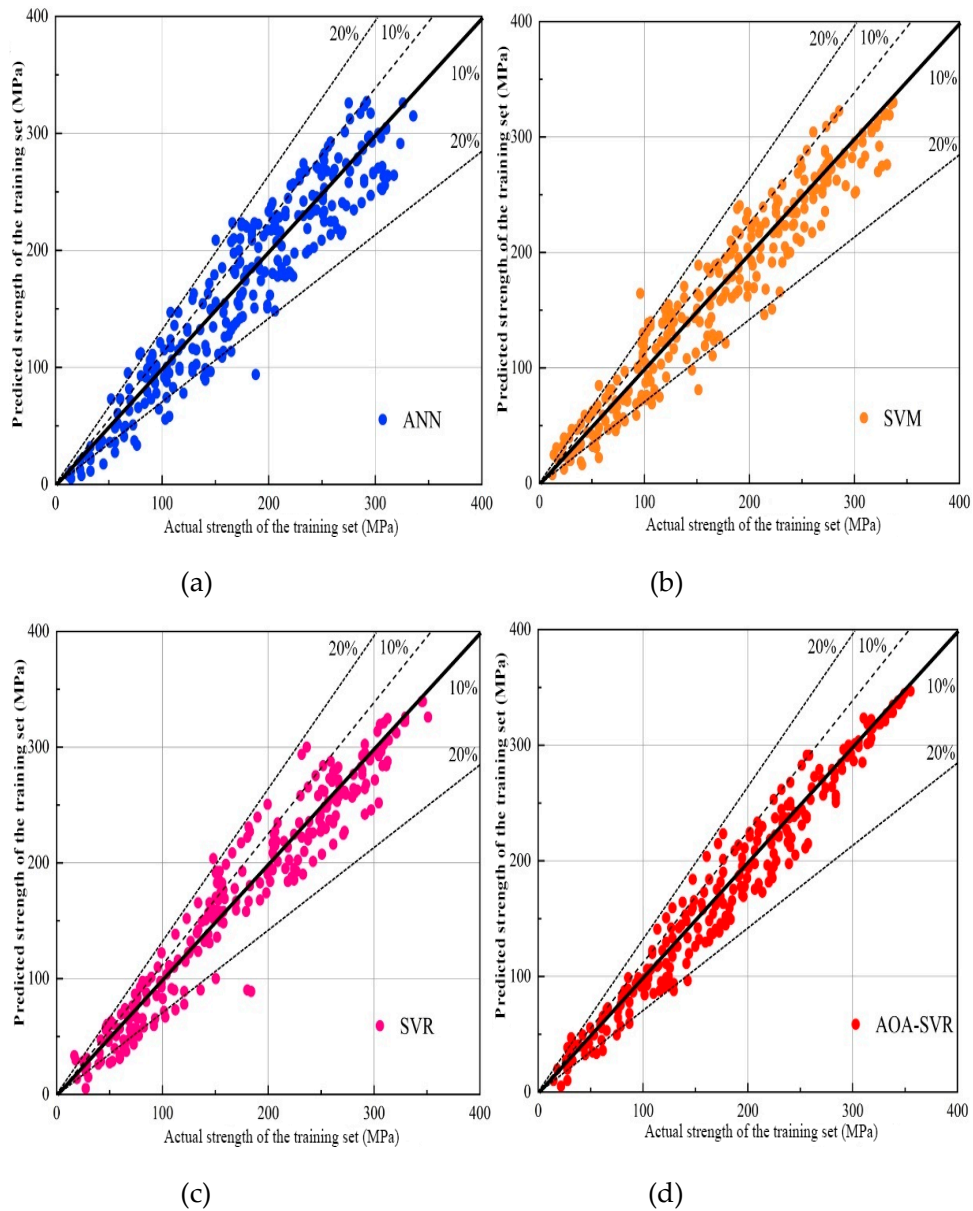


Figure 5. Regression diagrams of ANN, SVM, SVR, and AOA-SVR models during the training phase.

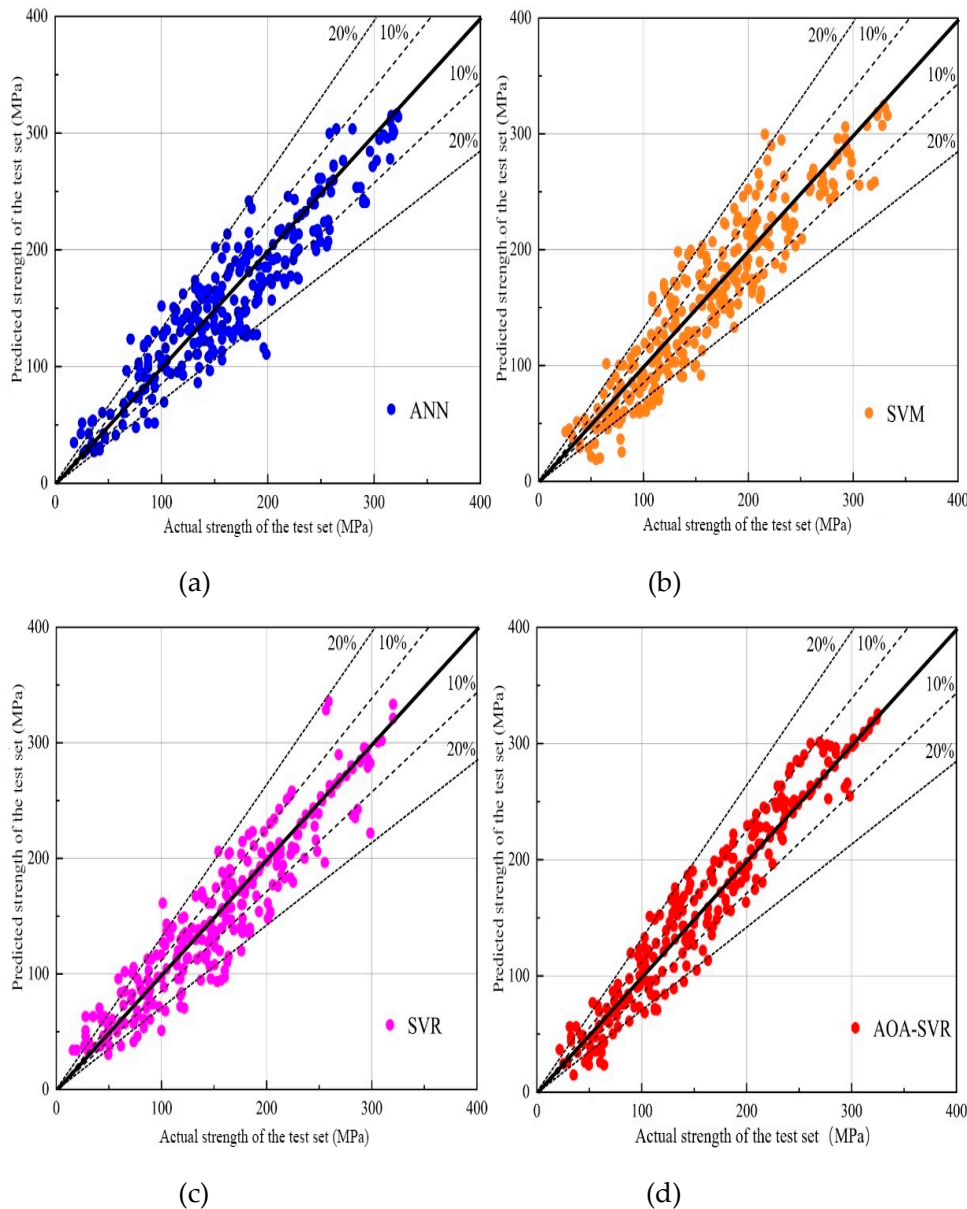


Figure 6. Regression diagrams of ANN, SVM, SVR, and AOA-SVR models during the test phase.

4.4.2. Model Explanation

In this study, the SHapley Additive exPlanations (SHAP) method is utilized to explain the model prediction results. The contribution analysis of the prediction results based on SHAP values can be divided into two levels according to the established model. Figures 7 and 8 provide a global interpretation of the AOA-SVR model. The results indicate that cement content has the most significant impact on the mechanical properties of UHPC, while slag powder has the least effect.

Figure 11 illustrates the distribution of SHAP values for each characteristic parameter and indicates their corresponding influence trends. The analysis reveals that higher values of steel fiber content, cement content, fly ash content, and silica fume content are associated with larger SHAP values. Conversely, higher values of water content, superplasticizers content, and slag powder content correspond to smaller SHAP values. This indicates that steel fiber content, cement content, fly ash content, and silica fume content are positively correlated with compressive strength, whereas water content, superplasticizers content, and slag powder content are negatively correlated. This detailed SHAP analysis further demonstrates the reliability and robustness of machine learning methods for predicting the compressive strength of UHPC.

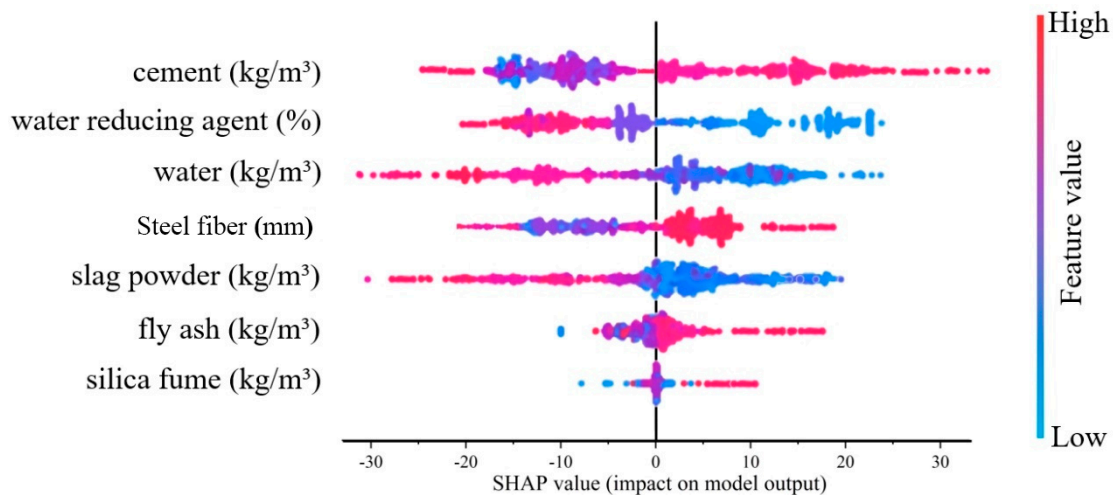


Figure 7. Evaluation summary chart.

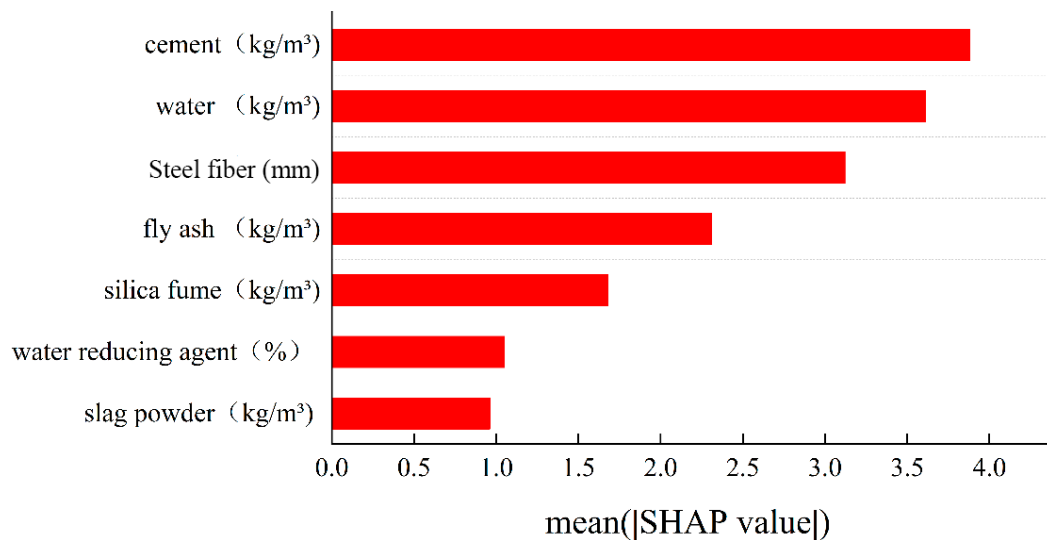


Figure 8. Feature importance.

5. Conclusions

This study examined the impact of both single factors and combined factors on UHPC performance using experimental data. These innovations effectively address previous limitations, such as using different machine learning and deep learning for predicting concrete properties. Based on analyzing these factors both in isolation and combination, the study provides a comprehensive understanding of their roles and interactions, which are often complex and non-linear. The following results are obtained in this study:

(1) Through meticulous data processing and algorithm optimization, three-dimensional graphics were utilized to visually display the impact of various influencing factors on the compressive strength of UHPC. This approach allows for the optimization of material ratios in the design and construction of UHPC structures to achieve desired performance goals in practical projects.

(2) The AOA-SVR hybrid model outperforms the ANN, SVM, and SVR single models, achieving the highest prediction accuracy with $R^2 = 0.9628$. In addition, the very low (RMSE = 1.5779 MPa, and MAE = 1.1796 MPa) values on training and test sets indicate that no overfitting was produced.

(3) Based on the SHAP evaluation summary and feature importance analysis, followed by AOA-SVR hybrid model, it indicates that cement content was the most influential variable on the compressive strength of UHPC, while slag powder had the least influence.

Author Contributions: W.L.Y. and D.D.: conceptualization. W.L.Y., L.L. and D.D.: methodology. W.L.Y., L.L., L.B. and C.Z.Y.: software. W.L.Y., L.L., D.D., L.B. and C.Z.Y.: validation. L.L. and D.D.: investigation. D.D.: data curation. L.L.: writing—original draft preparation. W.L.Y., L.L., D.D., L.B., and C.Z.Y.: writing—review and editing. W.L.Y., and L.B.: visualization. W.L.Y.: supervision. All authors have read and agreed to the published version of the manuscript.

Funding: Project supported by the National Natural Science Foundation of China (Grant Nos. 12102269), General Fund of Liaoning provincial Science and Technology Fund 2022-MS-402. Besides, this work was funded by Shenyang ,key laboratory of safety evaluation and disaster prevention of engineering structures (grant number S230184).

Informed Consent Statement: Informed consent was obtained from all subjects involved in the study.

Data Availability Statement: The original contributions presented in this study are included in the article, and further inquiries can be directed to the corresponding author.

Acknowledgments: A great thank you to all collaborators for their availability and contribution to this study.

Conflicts of Interest: The authors declare no conflicts of interest.

References

1. AMRAN M, HUANG Shan-shan, ONAIZI A M, et al.Recent trends in ultra-high performance concrete (UHPC): Current status, challenges, and future prospects[J]. *Construction and Building Materials*, 2022, 352. DOI: 10.1016/j.CONBUILDMAT.2022.129029.
2. FAN Ding-qiang, YU Rui, FU Shi-yuan, et al.Precise design and characteristics prediction of Ultra-High Performance Concrete (UHPC) based on artificial intelligence techniques[J]. *Cement and Concrete Composites*, 2021, 122(prepublish):104171-.DOI:10.1016/j. CEMCONCOMP.2021.104171.
3. MURTAGH N, SCOTT L, FAN Jing-li, Sustainable and resilient construction: Current status and future challenges[J]. *Journal of Cleaner Production*, 2020, 268 (prepublish).DOI: 10.1016/j.jclepro.2020.122264.
4. SHI Cai-jun, WU Ze-mei, XIAO Jian-fan, et al. A review on ultra high performance concrete: Part I. Raw materials and mixture design[J]. *Construction and Building Materials*, 2015, 101741-751. DOI: 10.1016/j.conbuildmat.2015.10.088
5. MARANI A, JAMALI A, NEHAI M L.Predicting Ultra-High-Performance Concrete Compressive Strength Using Tabular Generative Adversarial Networks.[J]. *Materials (Basel,Switzerland)* ,2020,13(21):4757-4757.DOI:10.3390/ma13214757.
6. HUANG Yan-bo.Advances in Artificial Neural Networks-Methodological Development and Application[J]. *Algorithms*, 2009, 2(3):973. DOI:10.3390/ALGOR2030973
7. SARKER I H, JANICKE H, FERRAG M A, et al. Multi-aspect rule-based AI: Methods, taxonomy, challenges and directions towards automation, intelligence and transparent cybersecurity modeling for critical infrastructures[J]. *Internet of Things*, 2024, 25:101110-. DOI: 10.1016/j.IOT.2024.101110.
8. OTCHERE D A, ARBI G T, GHOLAMI R, et al. Application of supervised machine learning paradigms in the prediction of petroleum reservoir properties: Comparative analysis of ANN and SVM models[J]. *Journal of Petroleum Science and Engineering*, 2020, 108182-. DOI: 10.1016/j.PETROL.2020.108182.
9. TANVESH D, HARISH N, PRASHANTH J, et al. A review of soft computing techniques in predicting the compressive strength of concrete and the future scope[J]. *Innovative Infrastructure Solutions*, 2023, 8(6). DOI: 10.1007/S41062-023-01150-5.
10. MANA A, MAJID Khan, MUHAMMAD F, et al. Predictive modeling for compressive strength of 3D printed fiber-reinforced concrete using machine learning algorithms[J]. *Case Studies in Construction Materials*, 2024, 20:e02728-. DOI: 10.1016/J.CSCM.2023.E02728
11. Joaquín A. Study of nonlinear relationships between dosage mixture design and the compressive strength of UHPC[J]. *Case Studies in Construction Materials*, 2022, 17.DOI: 10.1016/J.CSCM.2022.E01228.
12. HENSON M A. Nonlinear model predictive control: current status and future directions[J]. *Computers and Chemical Engineering*, 1998, 23(2): 187-202. DOI: 10.1016/S0098- 1354(98)00260-9.
13. GOLAFSHANI E M, BEHNOOD Ali, KIM T, et al. Metaheuristic optimization based- ensemble learners for the carbonation assessment of recycled aggregate concrete[J]. *Applied Soft Computing*, 2024, 159:111661-. DOI:10.1016/J.ASOC.2024.111661.
14. SULTAN Y B, SUMIT K, NATEE P, et al. A novel hybrid arithmetic optimization algorithm for solving constrained optimization problems[J]. *Knowledge-Based Systems*, 2023, 271.DOI: 10.1016/J.KNOSYS.2023.110554.
15. CAO Li, CHEN Hai-shao, CHEN Yao-dan, et al. Bio-Inspired Swarm Intelligence Optimization Algorithm-Aided Hybrid TDOA/AOA-Based Localization[J]. *Biomimetics (Basel, Switzerland)*, 2023, 8(2). DOI: 10.3390/BIOMIMETICS8020186.

16. MUHAMMED Y, SONER K, SERPIL A, et al. A new hybrid approach based on AOA, CNN and feature fusion that can automatically diagnose Parkinson's disease from sound signals: PDD-AOA-CNN[J]. *Signal, Image and Video Processing*, 2023, 18(2):1227-1240.DOI: 10.1007/S11760-023-02826-2.
17. LI Chuan-qi, MEI Xian-cheng. Application of SVR models built with AOA and Chaos mapping for predicting tunnel crown displacement induced by blasting excavation[J]. *Applied Soft Computing*, 2023, 147. DOI: 10.1016/J.ASOC.2023.110808.
18. YAO Hang, ZHANG Kai-fu, CHENG Hui, et al. An adaptive modelling approach using a novel modified AOA/SVR for prediction of drilling-induced delamination in CFRP/Ti stacks[J]. *Journal of Manufacturing Processes*, 2023, 102:259-274. DOI: 10.1016/J.JMAPRO.2023.07.045.
19. NGUYEN T T, THAI H T, NGO T.Effect of steel fibers on the performance of an economical ultra-high strength concrete[J]. *Special Theme: Sustainability of Concrete Structures*, 2023, 24(2): 2327-2341.
20. JIN Liu, ZHANG Ren-bo, TIAN Yu-dong, et al. Experimental investigation on static and dynamic mechanical properties of steel fiber reinforced ultra-high-strength concretes[J]. *Construction and Building Materials*, 2018, 178:102-111. DOI: 10.1016/j.conbuildmat. 2018.05.152.
21. SONG Yang, ZHAO Jun, OSTROWSKI K A, et al. Prediction of Compressive Strength of Fly-Ash-Based Concrete Using Ensemble and Non-Ensemble Supervised Machine-Learning Approaches[J]. *Applied Sciences*, 2021, 12(1):361-361.DOI: 10.3390/APP12010361.
22. GRAYBEAL B A. Practical Means for Determination of the Tensile Behavior of Ultra-High Performance Concrete[J]. *Journal of ASTM International*, 2006, 3(8):100387-100387. DOI: 10.1520/JAI100387.
23. SCHEYDT J C, Müller H S. Microstructure of ultra high performance concrete (UHPC) and its impact on durability[C]//*Proceedings of the 3rd international symposium on uhpc and nanotechnology for high performance construction materials*, Kassel, Germany. 2012: 349-356.
24. GRAYBEAL B A, HARTMANN J L. Strength and durability of ultra-high performance concrete[C]//*Concrete Bridge Conference*. Portland Cement Association, Washington, DC, 2003: 20.
25. ALI A, CANH N D, José R. Martí-Vargas, et al. Mixture-proportioning of economical UHPC mixtures[J]. *Journal of Building Engineering*, 2020, 27:100970-100970. DOI:10.1016/j.job.2019.100970
26. SOBUZ H R, VISINTIN P , MOHAMED M S, et al. Manufacturing ultra-high performance concrete utilising conventional materials and production methods[J]. *Construction and Building Materials*, 2016, 111: 251-261. DOI: 10.1016/j.conbuildmat.2016.02.102.
27. SHI Ye, LONG Guang-cheng, MA Cong, et al. Design and preparation of ultra-high performance concrete with low environmental impact[J]. *Journal of Cleaner Production*, 2019, 214:633-643.DOI: 10.1016/j.jclepro.2018.12.318.
28. Akça K R, IPEK M. Effect of different fiber combinations and optimisation of an ultra-high performance concrete (UHPC) mix applicable in structural elements[J]. *Construction and Building Materials*, 2022, 315: 125777.
29. RONANKI V S, AALETI S. Experimental and analytical investigation of UHPC confined concrete behavior[J]. *Construction and Building Materials*, 2022, 325. DOI: 10.1016/J.CONBUILDMAT.2022.126710.
30. FAN Ding-qiang, ZHU Jin-yun, FAN Meng-xin, et al. Intelligent design and manufacturing of ultra-high performance concrete (UHPC) – A review[J]. *Construction and Building Materials*, 2023, 385.DOI:10.1016/J.CONBUILDMA T.2023.131495.
31. ALSALMAN A, DANG C N, HALE W M, et al. Development of ultra-high performance concrete with locally available materials[J]. *Construction and Building Materials*, 2017, 133:135-145.DOI: 10.1016/j.conbuildmat.2016.12.040.
32. FAN Ding-qiang, YU Rui, FU Shi-yuan, et al. Precise design and characteristics prediction of Ultra-High Performance Concrete (UHPC) based on artificial intelligence techniques[J]. *Cement and Concrete Composites*, 2021, 122:104171-. DOI: 10.1016/J.CEMCONCOMP. 2021.104171.
33. YANG Rui, YU Rui, SHUI Zhong-he, et al. Low carbon design of an Ultra-High Performance Concrete (UHPC) incorporating phosphorous slag[J]. *Journal of Cleaner Production*, 2019, 240:118157-118157. DOI:10.1016/j.jclepro.2019. 118157.
34. FENG Shuo, XIAO Hui-gang, MA Ming-lei, et al. Experimental study on bonding behaviour of interface between UHPC and concrete substrate[J]. *Construction and Building Materials*, 2021, 311.DOI:10.1016/J.CONBUILDMA T.2021.125360.
35. YU R, SPIESZ P, BROUWERS H J H, et al. Development of an eco-friendly Ultra-High Performance Concrete (UHPC) with efficient cement and mineral admixtures uses[J]. *Cement and Concrete Composites*, 2015, 55: 383-394. DOI: 10.1016/j.cemconcomp. 2014.09.024.
36. MAGUREANU C, SOSA I, et al. Mechanical Properties and Durability of Ultra-High-Performance Concrete[J]. *Materials Journal*, 2012, 109(2).
37. LI P P, YU QL, BROUWERS H J H, et al. Effect of coarse basalt aggregates on the properties of Ultra-high Performance Concrete (UHPC)[J]. *Construction and Building Materials*, 2018, 170:649-659.DOI: 10.1016/j.conbuildmat.2018.03.109.

38. XIE T, FANG C, MOHAMAD M S, et al. Characterizations of autogenous and drying shrinkage of ultra-high performance concrete (UHPC): An experimental study[J]. *Cement and Concrete Composites*, 2018, 91:156-173. DOI: 10.1016/j.cemconcomp.2018.05.009.
39. OUYANG Xue, SHI Cai-jun, WU Ze-mei, et al. Experimental investigation and prediction of elastic modulus of ultra-high performance concrete (UHPC) based on its composition[J]. *Cement and Concrete Research*, 2020, 138. DOI: 10.1016/j.cemconres.2020.106241.
40. ALKAYSI M, ELTAWIL S, LIU Zhi-chao, et al. Effects of silica powder and cement type on durability of ultra high performance concrete (UHPC)[J]. *Cement and Concrete Composites*, 2016, 66:47-56. DOI:10.1016/j.cemconcomp.2015.11.005.
41. TEICHMANN T, Schmidt M. Influence of the packing density of fine particles on structure, strength and durability of UHPC[C]//International symposium on ultra high performance concrete. 2004: 313-323.
42. MA J, ORGASS M, DEHN F, et al. Comparative investigations on ultra-high performance concrete with and without coarse aggregates[C]//International symposium on ultra high performance concrete, Kassel, Germany. 2004: 205-212.
43. JIN B K, KISS S, KIP P, et al. Mechanical Properties of Ultra High Strength Concrete Using Ternary Blended Cement[J]. *Journal of the Korea institute for structural maintenance inspection*, 2012, 16(6):56-62. DOI:10.11112/jksmi.2012.16.6.056.
44. DING Meng-xi, YU Rui, FENG Yuan, et al. Possibility and advantages of producing an ultra-high performance concrete (UHPC) with ultra-low cement content[J]. *Construction and Building Materials*, 2021, 273. DOI: 10.1016/j.conbuildmat.2020.122023.
45. XUE Jun-qing, BRISEHELLA B, HUANG Fu-yun, et al. Review of ultra-high performance concrete and its application in bridge engineering[J]. *Construction and Building Materials*, 2020, 260. DOI: 10.1016/j.conbuildmat.2020.119844.
46. HOU Dong-shuai, WU Di, WANG Xin-peng, et al. Sustainable use of red mud in ultra-high performance concrete (UHPC): Design and performance evaluation[J]. *Cement and Concrete Composites*, 2021, 115:103862-. DOI:10.1016/j.cemconcomp.2020.103862.
47. YANG Rui, YU Rui, SHUI Zhong-he, et al. The physical and chemical impact of manufactured sand as a partial replacement material in Ultra-High Performance Concrete (UHPC)[J]. *Cement and Concrete Composites*, 2019, 99:203-213. DOI:10.1016/j.cemconcomp.2019.03.020.
48. WANG Xin-peng, YU Rui, SONG Qiu-lei, et al. Optimized design of ultra-high performance concrete (UHPC) with a high wet packing density[J]. *Cement and Concrete Research*, 2019, 126: 105921-105921. DOI:10.1016/j.cemconres.2019.105921.
49. WU Ze-mei, SHI Cai-jun, HE Wen, et al. Static and dynamic compressive properties of ultra-high performance concrete (UHPC) with hybrid steel fiber reinforcements[J]. *Cement and Concrete Composites*, 2017, 79:148-157. DOI: 10.1016/j.cemconcomp.2017.02.010.
50. FEHLING E, Schmidt M, Walraven J, et al. Ultra-high performance concrete UHPC[J]. *Ernst & Sohn: Berlin, Germany*, 2014: 25-32.
51. ZHANG Hong-ru, JI Tao, ZENG Xue-peng, et al. Mechanical behavior of ultra-high performance concrete (UHPC) using recycled fine aggregate cured under different conditions and the mechanism based on integrated microstructural parameters[J]. *Construction and Building Materials*, 2018, 192:489-507. DOI: 10.1016/j.conbuildmat.2018.10.117.
52. ARORA A, YAO Yi-ming, MOBASHER B, et al. Fundamental insights into the compressive and flexural response of binder- and aggregate-optimized ultra-high performance concrete (UHPC)[J]. *Cement and Concrete Composites*, 2019, 98:1-13. DOI:10.1016/j.cemconcomp.2019.01.015.
53. DARSSNI R, RANJAN P P, KUMAR K S, et al. Influence of fibers on fresh and hardened properties of Ultra High Performance Concrete (UHPC)—A review[J]. *Journal of Building Engineering*, 2022, 57. DOI: 10.1016/j.jobe.2022.104922.
54. YU Zhi-hui, WU Li-shan, YUAN Zhen, et al. Retraction notice to “Mechanical properties, durability and application of ultra-high-performance concrete containing coarse aggregate (UHPC-CA): A review”[Constr. Build. Mater. 334 (2022) 127360][J]. *Construction and Building Materials*, 2023, 395. DOI: 10.1016/j.conbuildmat.2023.132232.
55. SU Yu, WU Cheng-qing, LI Jun, et al. Development of novel ultra-high performance concrete: From material to structure[J]. *Construction and Building Materials*, 2017, 135:517-528. DOI: 10.1016/j.conbuildmat.2016.12.175.
56. GONG Ji-hao, MA Yu-wei, FU Ji-yang, et al. Utilization of fibers in ultra-high performance concrete: A review[J]. *Composites Part B*, 2022, 241. DOI: 10.1016/j.compositesb.2022.109995.
57. WANG Chong, YANG Chang-hui, LIU Fang, et al. Preparation of Ultra-High Performance Concrete with common technology and materials[J]. *Cement and Concrete Composites*, 2012, 34(4):538-544. DOI: 10.1016/j.cemconcomp.2011.11.005.

58. SBIA L A, PEYVANDI A, LU J, et al. Production methods for reliable construction of ultra-high-performance concrete (UHPC) structures[J]. *Materials and Structures*, 2017, 50(1).DOI: 10.1617/s11527-016-0887-4.
59. AKHNOUKH A K, BUCKHALTER C. Ultra-High-Performance Concrete: Constituents, Mechanical Properties, Applications and Current Challenges[J]. *Case Studies in Construction Materials*, 2021, :e00559-. DOI: 10.1016/J.CSCM.2021.E00559.
60. FARZAD M, SHAFIEIFAR M, AZIZINAMINI A, et al. Experimental and numerical study on bond strength between conventional concrete and Ultra High-Performance Concrete (UHPC)[J]. *Engineering Structures*, 2019, 186: 297-305. DOI:10.1016/j.engstruct. 2019.02.030.
61. GU Chun-Ping, YE Guang, SUN Wei, et al. Ultrahigh performance concrete-properties, applications and perspectives[J]. *Science China Technological Sciences*, 2015, 58(4):587-599.DOI: 10.1007/s11431-015-5769-4.
62. ABBAS S, NEHDI M L, SALEEM M A, et al. Ultra-High Performance Concrete:Mechanical Performance, Durability, Sustainability and Implementation Challenges[J]. *International Journal of Concrete Structures and Materials:International Journal of Concrete Structures and Materials*, 2016, 10(3): 271-295.DOI: 10.1007/s40069-016-0157-4.

Disclaimer/Publisher's Note: The statements, opinions and data contained in all publications are solely those of the individual author(s) and contributor(s) and not of MDPI and/or the editor(s). MDPI and/or the editor(s) disclaim responsibility for any injury to people or property resulting from any ideas, methods, instructions or products referred to in the content.